

## Complexation Kinetics of Copper(II) and Nickel(II) with Macrocycles: Identification of an Outer-Sphere Chelate Effect

Nichola McCann, Geoffrey A. Lawrance, Yorck-Michael Neuhold, and Marcel Maeder\*

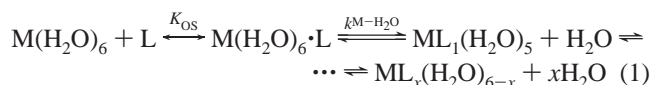
University of Newcastle, Newcastle NSW 2308, Australia

Received November 6, 2006

Ligand-protonation constants and complexation kinetics of differently protonated forms of 10-methyl-1,4,8,12-tetraazacyclopentadecan-10-amine, 1,4,8,12-tetraazacyclopentadecane, and 1,4,8,12-tetraazacyclopentadecan-10-carboxylic acid with Cu(II) and Ni(II) in aqueous solution have been determined. These results are combined with a wide range of published complexation rate constants of partially protonated macrocyclic ligands with the same metal ions. Insight is gained into the electrostatic effects and the outer-sphere interaction of partially protonated ligands with aquated metal ions. An outer-sphere chelate effect has been ascertained.

### Introduction

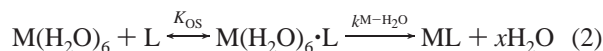
It is generally accepted that complexation of a metal ion by a multidentate ligand in aqueous solution occurs in several steps, as shown in eq 1, where all charges have been omitted for clarity.<sup>1</sup>



(We use the  $\leftrightarrow$  arrow to represent essentially instantaneous, kinetically unobservable equilibria and the  $\rightleftharpoons$  arrows for slow equilibria that are, at least theoretically, observable.) With the assumption of octahedral coordination,  $\text{ML}_x(\text{H}_2\text{O})_{6-x}$  represents the complex with the multidentate ligand coordinated at  $x$  sites with  $(6 - x)$  coordinated water molecules left in the octahedral complex. The first step involves the outer-sphere interaction of the aquated metal ion,  $\text{M}(\text{H}_2\text{O})_6$ , with the ligand, L, to form an outer-sphere complex,  $\text{M}(\text{H}_2\text{O})_6 \cdot \text{L}$ . This reaction is a fast, essentially instantaneous equilibrium which is quantitatively defined by the outer-sphere stability constant,  $K_{\text{OS}}$ . The results of a recent quantum mechanical study on the metal complex formation with simple mono- and bidentate ligands are entirely consistent with the above mechanism.<sup>2</sup> The second step is a ligand-

exchange reaction where one coordinated water molecule is replaced by the first coordinating Lewis base site of the ligand. This step is rate-determining and is controlled by the water-exchange rate,  $k^{\text{M}-\text{H}_2\text{O}}$ , of the hexaqua complex. The subsequent steps, the replacement of more coordinated water molecules by additional ligand sites, are much faster, and consequently they are usually not observable.

All steps in mechanism 1 are reversible reactions. In the case of macrocyclic ligands, the stability constants of the resultant complexes are very high, and so complex formation at sufficiently high pH can be regarded as irreversible. Omitting the water molecules still coordinated to the complex (correctly, ML should be written as  $\text{ML}_x(\text{H}_2\text{O})_{6-x}$ ) and due to the difficulty of detecting the secondary water–ligand-exchange reactions, the observable reaction reduces to



Under most conditions, the reaction scheme reduces to one kinetically observable second-order reaction



where the observed second-order rate constant  $k^{\text{M}+\text{L}}$  is the product of  $K_{\text{OS}}$  and  $k^{\text{M}-\text{H}_2\text{O}}$ .

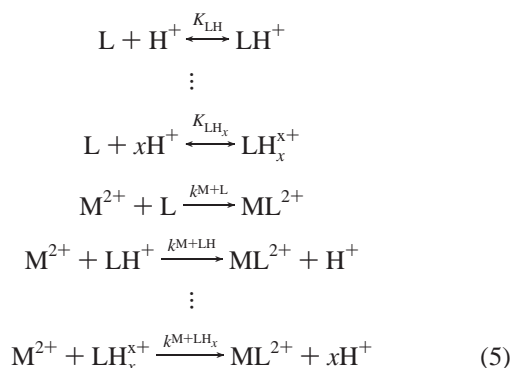
$$k^{\text{M}+\text{L}} = K_{\text{OS}}k^{\text{M}-\text{H}_2\text{O}} \quad (4)$$

In aqueous solution this system of reactions is tremendously complicated by the presence of protonation equilibria. The aquated metal ion can undergo hydrolysis, and most ligands are weak Brønsted bases and thus will be involved

\* To whom correspondence should be addressed. E-mail: marcel.maeder@newcastle.edu.au.

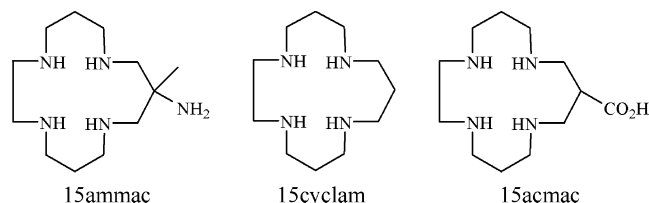
(1) Eigen, M. In *Advances in the Chemistry of the Coordination Compounds*; Kirshner, S., Ed.; The Macmillan Co.: New York, 1961; p 373.  
(2) Vallet, V.; Wahlgren, U.; Grenthe, I. *J. Am. Chem. Soc.* **2003**, *125*, 14941–14950.

in pH-dependent protonation equilibria. Equation 5 is a general representation of the protonation equilibria and the complexation reactions of the differently protonated ligands with the metal ion. The scheme describes the coordination kinetics in a slightly acidic aqueous solution where hydrolysis of the metal ion does not need to be considered.  $M^{2+}$  represents



the hexaquo complex and  $k^{M+LH_x}$  is the observable rate constant for the reaction with the  $x$  times protonated ligand; refer to eq 3.  $k^{M+LH_x}$  is the product of the outer-sphere equilibrium constant  $K_{OS}^{M+LH_x}$  for the formation of the outer-sphere complex  $M(H_2O)_6^{2+} \cdot LH_x$  multiplied by the water-exchange rate constant. Depending on the pH range investigated, several of the complexation reactions in the scheme as well as different protonation equilibria are not observed and thus their constants are not defined.

There is a wealth of reported data on the kinetics of copper(II) and nickel(II) complexation by polyamine macrocycles, and in this contribution we add the rates for the complex formation kinetics of 10-methyl-1,4,8,12-tetraazacyclopentadecan-10-amine (15ammac), 1,4,8,12-tetraazacyclopentadecan-10-carboxylic acid (15acmac) and 1,4,8,12-tetraazacyclopentadecane (15cyclam) with both metal ions.



The combination of these results with a wide collection of published rate constants allows detailed insight into the interaction of partially protonated macrocyclic ligands with metal ions and in particular into how the outer-sphere complexation properties of partially protonated ligands are influenced by the charge and the number of free, unprotonated ligand sites. This insight is not restricted to complexation reactions, and it is pertinent to most interactions between charged species in aqueous solution.

## Experimental Section

The hydrochloride salts of 15ammac and 15acmac were prepared as described previously.<sup>3–5</sup> The free base of 15cyclam was purchased from Aldrich. Copper(II) perchlorate hexahydrate and

nickel(II) perchlorate hexahydrate were of AR grade, and all metal solutions were standardized prior to use. All other chemicals were of analytical grade and were used without further purification. The ionic strength of all solutions was adjusted to 0.5 M with recrystallized  $NaClO_4$ . All reactions were thermostatted at 25 °C.

Ligand-protonation constants were determined by employing data collected by a fully computerized potentiometric titration setup comprising a Metrohm combined glass electrode (6.0234.100) read by a PCI-6014 NI-DAQ data acquisition board and a Metrohm 665 Dosimat buret. All titrations were performed under a nitrogen atmosphere; 3–20 mL of an approximately  $5 \times 10^{-3}$  M ligand solution containing 10–100% acid excess ( $HClO_4$ ) was titrated with a 0.1 M NaOH solution, typically in increments of 1–10  $\mu$ L.

The complex formation kinetics were measured under different levels of ligand excess (10% to 5-fold) and different initial concentrations of acid. The initial concentration of metal was approximately  $2 \times 10^{-3}$  M for Cu/15ammac and Cu/15acmac measurements,  $4 \times 10^{-3}$  M for Cu/15cyclam measurements,  $5 \times 10^{-3}$  M for Ni/15ammac and Ni/15acmac measurements, and  $2 \times 10^{-2}$  M for Ni/15cyclam measurements. The initial pH in the case of Cu(II) was 5.8 or lower and for Ni(II) it was 6.8 or lower to avoid the formation of metal–hydroxo complexes. At relatively high pH levels, the reactions are fast, and measurements were taken on an Applied Photophysics DX-17 stopped-flow spectrophotometer using the “point-by-point” method where kinetic traces were acquired individually over an appropriate wavelength range between 485 and 650 nm at 15 nm intervals for Cu(II) and between 365 and 625 nm at 15 nm intervals for Ni(II). Depending on the initial pH, most total reaction times were between 0.2 and 1000 s for both metal ions. The shorter stopped-flow measurements were acquired at 400 linearly spaced times, whereas measurements over 10 s were collected at 1000 logarithmically spaced times. One reaction of Ni(II) with 15acmac was acquired over a longer time scale on a Hitachi 220A UV–vis spectrophotometer after manual mixing (2100 s at 445–625 nm). Small inaccuracies in time due to the relatively slow scanning of the spectrophotometer were corrected by interpolation. For each metal/ligand system, all measurements were analyzed globally; i.e., all individual multi-wavelength data sets acquired under different initial conditions (ligand and proton concentrations) were fitted together, using a global model as represented in eq 5. All data fitting was done with Pro-Kineticist II.<sup>6</sup>

No pH buffers were used. The proton concentration is incorporated into the kinetic analysis software and computed as a function of the reaction time, continuously taking into account all protonation equilibria.<sup>6</sup> A table with the initial concentrations of ligand, metal, and protons and the pH range covered for each individual measurement is given in the Supporting Information.

## Results

Figure 1 displays original data and results of the analysis for the representative measurement of the reaction of Cu(II) with 15ammac at an initial pH of approximately 4.0 and a ligand-to-metal ratio L:M of  $\sim 5$ . The spectra were measured between 505 and 640 nm at 15 nm intervals over a total time interval of 0.2 s (part a). Also shown are the calculated

- (4) Lawrance, G. A.; O’Leary, M. A.; Skelton, B. W.; Woon, F.-H.; White, A. H. *Aust. J. Chem.* **1988**, *41*, 1533–1544.
- (5) Lawrance, G. A.; Skelton, B. W.; White, A. H.; Wilkes, E. N. *Aust. J. Chem.* **1991**, *44*, 1511–1522.
- (6) Maeder, M.; Neuhold, Y.-M.; Puxty, G.; King, P. *Phys. Chem. Chem. Phys.* **2003**, *5*, 2836–2841.

(3) Lawrance, G. A.; O’Leary, M. A. *Polyhedron* **1987**, *6*, 1291–1294.

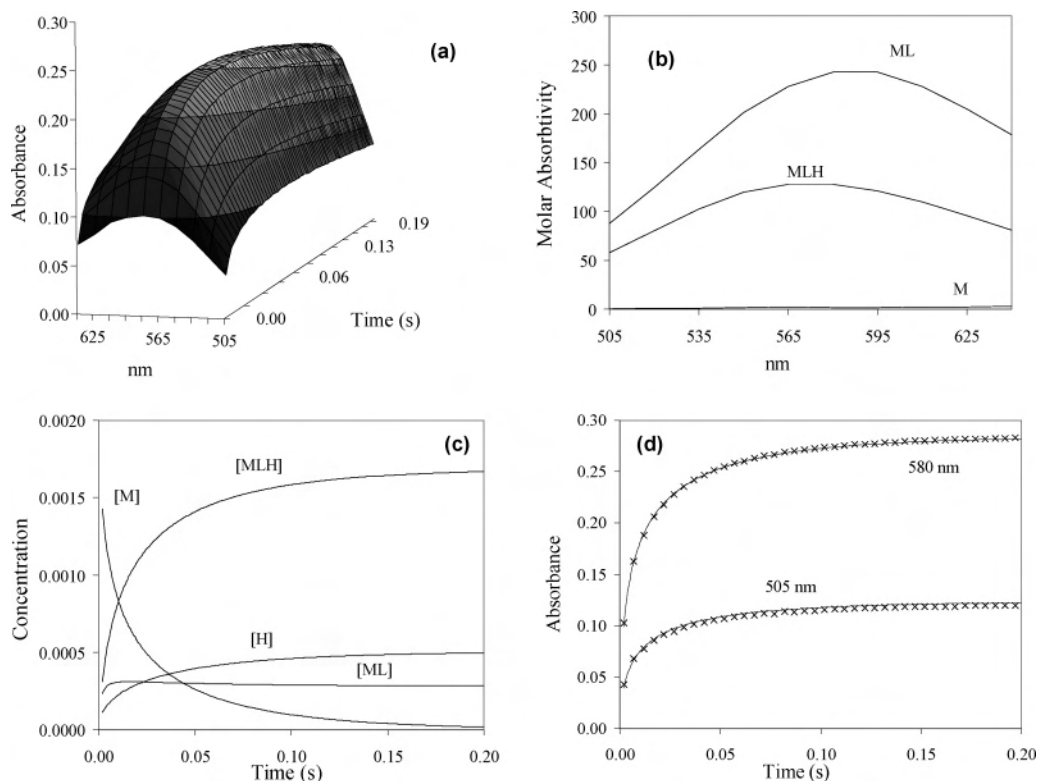


**Figure 1.** (a) Spectral changes associated with the reaction of  $\text{Cu}^{2+}$  with 15ammac in aqueous solution at an initial pH of 4.0; (b) calculated spectra; (c) concentration profiles of colored species and  $\text{H}^+$ ; and (d) comparison of measured (x) and calculated (solid line) absorbance at 505 and 580 nm.

spectra (maxima:  $\epsilon_{\text{ML}}(587 \text{ nm}) = 245 \text{ M}^{-1} \text{ cm}^{-1}$ ,  $\epsilon_{\text{MLH}}(572 \text{ nm}) = 129 \text{ M}^{-1} \text{ cm}^{-1}$ ) (part b). The reported maxima for the spectra are computed by quadratic interpolation through the available data points (see also Table 2), concentration profiles for all absorbing species present ( $\text{M} = \text{Cu}^{2+}$ ,  $\text{ML} =$  complex,  $\text{MLH} =$  protonated complex) (part c), and the comparison between measured and calculated kinetic traces at 505 and 580 nm (part d).

Most recorded data could be fitted to the basic model of eq 5. In some systems additional reactions were observed. Tetraaza macrocycles with a single pendant group can coordinate as pentadentate ligands or as tetradentate ligands with a protonated dangling arm, an equilibrium that has been identified in several systems.<sup>7</sup> In these cases, the reaction scheme in eq 5 has to be augmented by a secondary protonation equilibrium. Although this reaction involves the breaking of a coordination bond, the bond is weak and thus the reaction is expected to be fast. It has been possible to model it as a normal, instantaneous protonation equilibrium.



Spectral changes resulting from protonation and, thus, dissociation of the pendant arm are expected to be small for the carboxylate group, as the O-donor character remains at the substitution site; substitution of the amine group with a water molecule will induce larger spectral changes. In fact, we only observed the process in the case of 15ammac with both metal ions. With this ligand, the protonation involves

the transformation of the relatively strongly distorted  $\text{N}_5$  complex into a more symmetric and less-distorted square-planar  $\text{N}_4$  complex. The geometry changes are reflected in the absorption spectra of the species  $\text{ML}$  and  $\text{MLH}$ : for both metals, we observe a blue shift of the absorption maximum upon protonation and a lowering of the molar absorptivity due to the reduced distortion. We need to stress here that only global analysis of all measurements acquired at different initial proton concentrations (different pH ranges covered during the reaction) allows the robust detection of the protonation of the dangling arm.

In some systems, the initially formed complex underwent an observable first-order isomerization step, which was much slower in most instances. Again, such secondary isomerization steps have been observed before.<sup>7–10</sup>



In the case of  $\text{Cu}(\text{II})$ , the spectral changes associated with this slow step were very small and we could not determine a reliable rate constant. With  $\text{Ni}(\text{II})$ , spectral changes are more substantial; nevertheless, the reaction was clearly observable only for the acid pendant macrocycle 15acmac. Detailed kinetic analysis is very difficult, as the observed absorbance changes probably represent several isomerization steps that occur in parallel. As these reactions are not central to this study, we did not pursue this observation further.

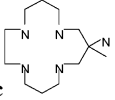
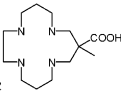
(7) Lye, P. G.; Lawrance, G.; Maeder, M. *J. Chem. Soc., Dalton Trans.* **2001**, 16, 2376–2382.

(8) Lindoy, L. F. *The Chemistry of Macrocyclic Ligand Complexes*; Cambridge University Press: Melbourne, Australia, 1989.

(9) Steinmann, W.; Kaden, T. A. *Helv. Chim. Acta* **1975**, 58, 1358–1366.

(10) Liang, B. F.; Margerum, D. W.; Chung, C. S. *Inorg. Chem.* **1979**, 18, 2001–2007.

**Table 1.** Ligand-Protonation Constants and Complexation Rate Constants for 15ammac, 15cyclam, and 15acmac

	 15ammac			 15cyclam			 15acmac		
	pot titration	Cu-kinetics	Ni-kinetics	pot titration	Cu-kinetics	Ni-kinetics	pot titration	Cu-kinetics	Ni-kinetics
$\log K_{LH}$	10.81 (0.3)			11.13 (4)			10.41 (4)		
$\log K_{LH2}$	9.75 (0.3)			9.97 (8)			9.62 (7)		
$\log K_{LH3}$	5.67 (0.4)			5.05 (9)	4.99 (0.8)		4.49 (8)	5.13 (0.2)	
$\log K_{LH4}$	3.2 (0.7)	3.36 (0.4)	3.20 (4)	3.52 (9)	3.68 (0.3)	3.18 (4)	3.52 (8)	3.47 (0.3)	
$\log K_{LH5}$	<2	2.00 (0.2)					<2		
$\log K_{MLH}$	4.13 (0.4)(Cu)	4.08(0.7)	5.07 (1)						
$k^{M+LH} [M^{-1}s^{-1}]$			$1.23(8) \times 10^4$		$1.04(4) \times 10^8$	$1.32(5) \times 10^2$			
$k^{M+LH2} [M^{-1}s^{-1}]$		$7.20(8) \times 10^5$	4.73 (2)		$3.54(4) \times 10^3$	$2.27(3) \times 10^{-2}$		$6.29(4) \times 10^4$	$3.17(1) \times 10^{-1}$
$k^{M+LH3} [M^{-1}s^{-1}]$		$1.86(2) \times 10^3$							
$k_{isom} [s^{-1}]$									$1.42(1) \times 10^{-3}$

**Table 2.** Spectra of Cu<sup>2+</sup> and Ni<sup>2+</sup> Complexes with 15ammac, 15cyclam, and 15acmac

	species	$\lambda_{max}$ ( $\epsilon$ ) [nm] [M <sup>-1</sup> cm <sup>-1</sup> ]	
		Cu(II)	Ni(II)
15ammac	ML	587 (245)	539 (7.2)
	MLH	572 (129)	534 (6.0)
15cyclam	ML	577 (158)	456 (48)
15acmac	ML	572 (137)	458 (3.9) 548 (4.6)
	ML*		550 (7.0)

Table 1 lists all results for the ligands 15ammac, 15cyclam, and 15acmac. The numbers in brackets represent the error estimates for the fitted parameters, computed in the normal way from the variance–covariance matrix.<sup>11</sup> Often, these error estimates are too small and not completely realistic. Error analysis of globalized data analyses is not well understood, and no attempts were made to improve the error analysis.

The ligand-protonation constants, as determined by potentiometric titrations, are all within the expected ranges. Those ligand-protonation equilibria that occur within the pH range covered by the kinetic measurements can be ascertained by the fitting of the kinetic data. Table 1 demonstrates excellent agreement between potentiometrically and kinetically determined protonation constants. The only exceptions are the protonations of 15acmac; for Ni(II), the pH range of the measurements does not cover the  $\log K_{LH2,3}$  values and thus they could not be fitted; no explanation can be given for the relatively large discrepancy for Cu(II).

In all analyses, the fitted spectra for the hexaqua metal ions and for the complexes were reasonable, thus supporting the suggested mechanism and the determined rate and protonation constants; see also Figure 1b for a graph of the

spectra of the Cu(II)/15ammac system. The values for  $\lambda_{max}$  and corresponding molar absorptivities (Table 2) have been obtained by quadratic interpolation through the available data points. No error estimates for  $\lambda_{max}$  and molar absorptivity are given. Error analysis of the fitted spectra, analyzed by secondary polynomial fitting, is difficult and has not been attempted.

### Outer-Sphere Interactions

The rate constants collected in Table 1 add to a large body of published values for the complexation reaction of macrocycles with Cu(II) and Ni(II). In this part we combine our results of the complexation kinetics of Cu and Ni with 15ammac, 15acmac, and 15cyclam with the kinetic data of Cu and Ni complexation with several other macrocyclic ligands (Supporting Information).

Figure 2 is a graphical representation of a wide collection for macrocyclic ligand complexation with Cu(II) and Ni(II). A few exceptions are not included in this figure; they will be discussed later. The ordinates of the markers are the logarithms of the observed second-order rate constants  $k^{M+LH_x}$  (see eq 5); the abscissas are the charges of the partially protonated ligands. The number of angles on the markers represents the number of unprotonated donor atoms on the ligand available to bind to a metal center. For example, for a polyamine ligand, a triangle with a 2+ charge represents a ligand with three unprotonated donor atoms and two protonated donor atoms; a monoangle (drop shape) in the 4+ column represents a ligand with one unprotonated donor atom and four protonated donor atoms. The only exception is 15acmac, with one negatively charged carboxylate group in the free ligand; for this ligand, the charge is one unit lower than the number of protonated sites.

A trendline (line of best fit) has been drawn for each group of ligands with the same number of available sites; the solid lines are for Cu(II) and the dotted ones are for Ni(II). The bold parts of the lines represent the range covered by the data, whereas the fine lines represent extrapolations. Table 3 collects the details of the fitted straight lines. The large error estimates for some values are mainly the result of large

(11) Bevington, P. R. *Data Reduction and Error Analysis for the Physical Sciences*; McGraw-Hill: New York, 1969.

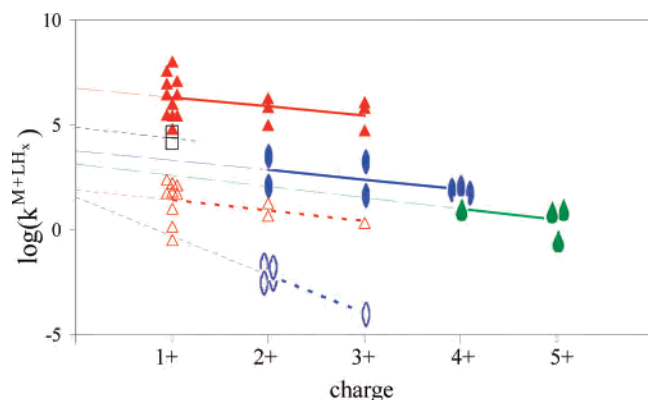


**Figure 2.** Plot of observed rate constants vs the charge of the partially protonated macrocyclic ligands. The number of angles of the markers indicates the number of unprotonated ligand sites. Full markers are for Cu(II) and outlined markers for the reactions with Ni(II). The lines are fitted to the groups of markers of the same kind, solid lines for Cu(II) and dotted lines for Ni(II). For clarity, some markers have been spread to the right and left of the actual charge on the abscissa. The lines are extrapolated to zero charge.

**Table 3.** Summary of the Straight-Line Fits of Figure 2: Slopes, Intercepts, and Calculated Outer-Sphere Equilibrium Constants

No. of unprot. donors	Cu(II)			Ni(II)	
	3▲	2●	1●	3△	2○
Charge range	+1...+3	+2...+4	+4...+5	+1...+3	+2...+3
Slope	-0.4 (3)	-0.5 (3)	-0.5 (9)	-0.5 (4)	-1.9 (5)
Intercept, $\log(k^{M+L})$	6.7 (5)	4 (1)	3 (5)	1.9 (6)	2 (1)
$\log(K_{OS})$	-2.6 (5)	-6 (1)	-6 (5)	-2.6 (6)	-3 (1)

extrapolations; some trendlines are additionally poorly defined, as only one marker is available at one end of the data range (e.g., the diangles for Ni(II)).

The added trendlines in Figure 2 reveal two prominent tendencies: (a) As the charge of the incoming ligand increases, the rate constant decreases (negative slope of the trendlines); and (b) the rate constant increases with the number of unprotonated donor atoms (trendlines in Figure 2 lie higher for a higher number of free ligand sites or number of corners on the markers). The first effect is to be expected; it is the observable result of the electrostatic repulsion between the metal ion and the variably protonated ligands with appropriate positive charges. The second effect is less transparent. Both warrant further investigation.

**Effect of the Number of Donors.** The complexation kinetics of unprotonated, neutral ligands (with the exception of 15acmac) with hexaquo metal ions is not directly observable. At pH values that are sufficiently high for complete deprotonation of the ligands, the hydrated metal ions are hydrolyzed to form hydroxo species or insoluble oxides and hydroxides. Extrapolation of the trendlines in Figure 2 to zero charge allows the estimation of these elusive rate constants  $k^{M+L}$ , collected in Table 3 as y intercepts. Water-exchange rates for Cu(II) and Ni(II) in aqueous solution are  $2 \times 10^9$  and  $3 \times 10^4 \text{ s}^{-1}$ , respectively.<sup>12–14</sup> It is

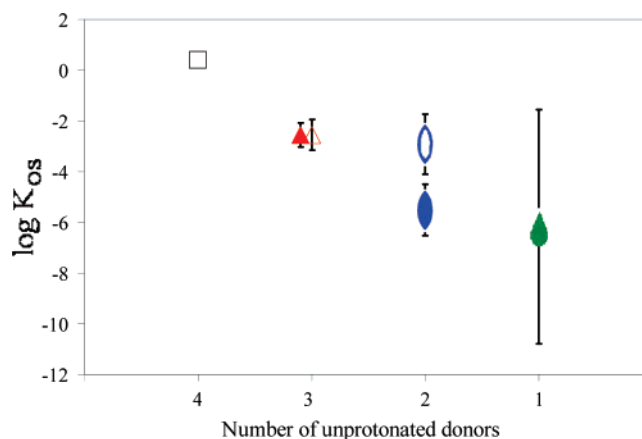


**Figure 3.** Plot of the logarithm of the outer-sphere equilibrium constants,  $\log K_{OS}$ , vs the number of unprotonated donor sites of the ligands. The full markers represent the values for  $\text{Cu}^{2+}$ , and the outlined markers represent the values for  $\text{Ni}^{2+}$ .

reasonable to assume that the water-exchange kinetics is not strongly affected by the outer-sphere complexation with a neutral ligand. According to eq 4, dividing the second-order rate constants by the water-exchange rate constants results in estimates for the outer-sphere equilibrium constants,  $K_{OS}$ . The computed values are listed in the last row of Table 3 and represented graphically in Figure 3.

The relationship between the number of free donor sites of the incoming ligands and the observed outer-sphere equilibrium constant is clearly apparent: the more free Lewis base sites on the ligand, the higher the  $K_{OS}$  values. The span of the different  $K_{OS}$  values of approximately 6 orders of magnitude cannot be explained by purely statistical factors. There is striking agreement for the well-defined  $K_{OS}$  values for the ligands with three available sites:  $\log(K_{OS}^{\text{Cu}+L}) = -2.6 \pm 0.5$ ,  $\log(K_{OS}^{\text{Ni}+L}) = -2.6 \pm 0.6$ . The equivalent values for ligands with two or one available site are not as well defined for reasons discussed earlier. The square in Figure 2 for the Ni(II) interaction with ligands with four free sites is based on only one set of data points in Figure 2. The intercept has been calculated using the average slope of the remaining trendlines. No error estimate is given for this marker.

We rationalize these observations with what we term an outer-sphere chelate effect. Most likely the attractive interaction is driven by the formation of hydrogen bridges between coordinated water molecules and free Lewis base sites on the ligands. Figure 4 is a schematic structure of the outer-sphere complex between Cu(II) and unprotonated cyclam. The static figure does not represent the dynamic nature of the outer-sphere interaction in aqueous solution. It is not expected that all four hydrogen bridges are formed at any time; fast fluctuation will average fewer bridges.

Such hydrogen bridges have been described before. The concept is similar to that of the internal conjugate base (ICB) mechanism, which has been used to explain the increased rate of reaction of unprotonated ethylenediamine with nickel compared with that of ammonia with nickel.<sup>15</sup> The ICB

(12) Makinen, W. B.; Pearlmutter, F. A.; Stuehr, J. *J. Am. Chem. Soc.* **1969**, *91*, 4083–4088.

(13) Pearlmutter, F. A.; Stuehr, J. *J. Am. Chem. Soc.* **1968**, *90*, 858–862.

(14) Margerum, D. W.; Rosen, H. M. *J. Am. Chem. Soc.* **1967**, *89*, 1088–1092.

(15) *Coordination Chemistry*; Martell, A. E., Ed.; American Chemical Society: Washington, DC, 1978; Vol. 2.

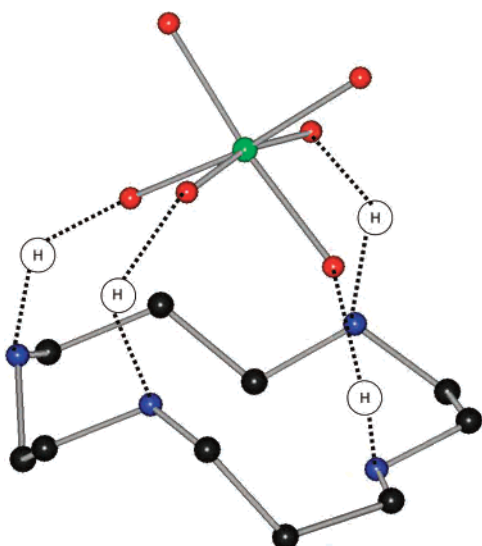


**Figure 4.** Schematic view of the outer-sphere complex between Cu(II) and deprotonated cyclam with hydrogen bridges.

mechanism suggests that the outer-sphere complex with ethylenediamine is stabilized by hydrogen bonding between an unprotonated amine and a water molecule coordinated to the metal ion. This results in a relatively large  $K_{OS}$ , which, in turn, increases the overall rate of the substitution reaction. It is expected that the presence of more donor atoms on the macrocyclic ligands studied results in the formation of additional hydrogen bridges. The outcome is a chelate effect in the formation of an outer-sphere complex.

Similar outer-sphere chelates have been previously identified through circular dichroism spectroscopic studies of the interaction between  $[\text{Co}(\text{NH}_3)_6]^{3+}$  and optically active anions, such as tartrate.<sup>16,17</sup> In these outer-sphere complexes, it is thought that the two carboxylate oxygens of the tartrate form hydrogen bonds to two adjacent ammonia hydrogens.

So far, we have concentrated on comparing estimated values of  $K_{OS}$  for neutral ligands. Similar trends are apparent in Figure 2 for the interaction of the metal ions with protonated ligands of different positive charges. They can be seen as the intercepts of the trendlines with ordinates at charges of 1+, 2+, etc. The water-exchange rates are influenced by the increasingly positively charged ligands in the outer-sphere complex. Although this effect cannot be estimated quantitatively, it is very likely to be relatively small. A table with all OS complexation constants (calculations based on the undisturbed water-exchange rates) is included in the Supporting Information.

**The Effect of Charge.** The charge of the partially protonated ligands has a distinct effect on the complex formation rate. This is clearly demonstrated by the consistent negative slope of the trendlines in Figure 2. In fact, it is surprising how similar these slopes are, and a closer inspection is warranted. The effect on the observed rate constant is the combined influence of the water-exchange rate and the outer-sphere equilibrium constant. The variations in  $k^{M+LH_x}$  cover several orders of magnitude, and although

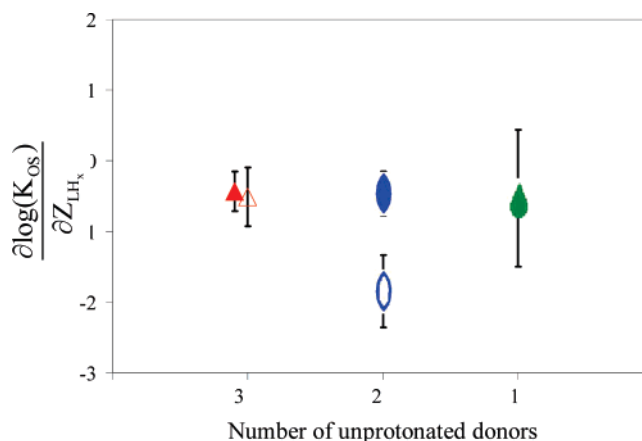


**Figure 5.** Effect of charge on the outer-sphere complexation of Cu (solid markers) and Ni (outlined markers) as a function of the number of unprotonated donors.

the water exchange will be influenced by the charge of the OS ligand, the effect will be relatively minor and the strength of the outer-sphere interaction must be the dominant effect for the observed rate constant.  $K_{OS}$  is determined by the charge and the formation of hydrogen bridges. Within one group of ligands with the same denticity (the same markers in Figure 2), the H-bridge interaction will be approximately constant and thus the charge remains as the determining factor.

Figure 5 displays the slopes of the trendlines of Figure 2, collected in Table 3. The figure reveals that all except one of the calculated experimental slopes are the same within 1 standard deviation. The outlying slope for ligands with two free sites for Ni(II) is very poorly defined and has already been identified as an outlier in Figure 3.

It is possible to estimate the electrostatic part of  $K_{OS}$  by equations derived by Fuoss<sup>18</sup> and expanded by Eigen and others<sup>19,20</sup> (eq 8, where  $N_A$  is Avogadro's number,  $Z_M$  is the formal charge of the metal ion,  $Z_{LH_x}$  is the formal charge on the OS complexing ligand,  $e_0$  is the electronic charge,  $\epsilon$  is the dielectric constant,  $\epsilon_0$  is the vacuum permittivity,  $k$  is the Boltzmann constant,  $T$  is the absolute temperature,  $a$  is the distance between the metal center and the unprotonated donors, and  $a'$  is the distance between the metal center and the protonated donors).

$$K_{OS} = \frac{4}{3} \pi a^3 N_A \exp\left(\frac{Z_M Z_{LH_x} e_0^2}{4 \pi a' \epsilon \epsilon_0 k T}\right) \quad (8)$$

Note that this form of the Fuoss equation was devised to describe ligands that contain one protonated donor atom and one unprotonated donor atom (as in monoprotated ethylenediamine). As none of the ligands studied herein contain only two donor atoms, the  $a$  and  $a'$  values are assumed to represent average values for the distances between the metal cation and all unprotonated donor atoms and the distances between the metal cation and all protonated donor atoms,

(16) Jonas, I.; Nordén, B. *Acta Chem. Scand., Ser. A* **1974**, 28, 289–293.

(17) Nordén, B. *Acta Chem. Scand.* **1972**, 111–126.

(18) Fuoss, R. M. *J. Am. Chem. Soc.* **1958**, 80, 5059–5061.

(19) Eigen, M.; Kruse, W.; Maass, G.; DeMaeyer, L. *Prog. React. Kinet.* **1964**, 2, 285–318.

(20) Rorabacher, D. B. *Inorg. Chem.* **1966**, 5, 1891–1899.

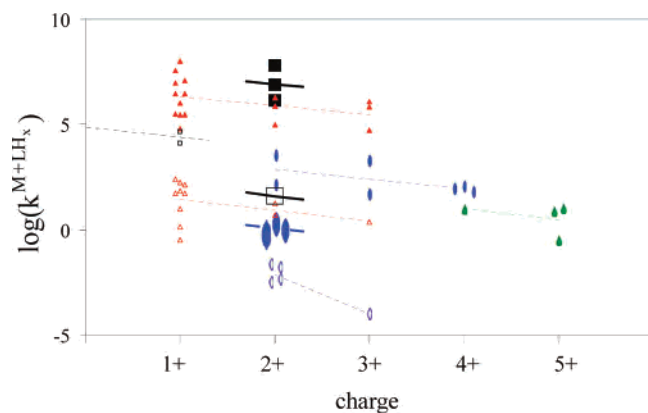


**Figure 6.** Plot of observed rate constants vs the ligand charge, including three sets of additional markers (represented by large symbols, squares for doubly protonated potentially hexadentate ligands, and diangles for doubly protonated cyclam analogues). For comparison, data from Figure 2 appear with small markers.

respectively. Some variation in ligand geometry with differing protonation may contribute to variability in data, so a higher level of definition is not warranted.

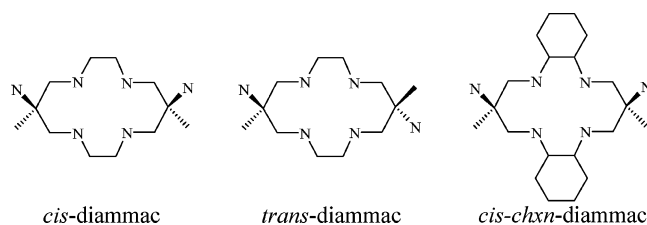
The slope of the trendlines of Figure 2 is the derivative of  $\log(K_{os})$  with respect to the charge of the partially protonated ligands,  $Z_{LH_x}$ . Derivation of eq 8 with respect to  $Z_{LH_x}$  results in

$$\frac{\partial \log(K_{os})}{\partial Z_{LH_x}} = \frac{Z_M e_0^2}{2.303 \times 4\pi a' \epsilon \epsilon_0 kT} \quad (9)$$

The only parameter undefined in eq 9 is  $a'$ , which is the distance of the metal from the protonated sites. The average slope of  $-0.5$  allows the computation of the distance  $a'$  to be approximately  $13 \text{ \AA}$ . Although this number should not be taken too literally, its value is consistent with the distances expected in loosely bound outer-sphere complexes, and this consistency supports the overall argument.

Discussed next are a few groups of ligands that do not fit the general trends revealed in Figure 2. These are highlighted in Figure 6 in full-size markers and bold trendlines; the data from Figure 2 are included in small symbols and light trendlines.

**Ligands with Two Pendant Arms.** In the series of macrocyclic ligands discussed here, there are three ligands based on the 14-cyclam backbone that feature two additional primary amines attached as pendant arms drawn below.



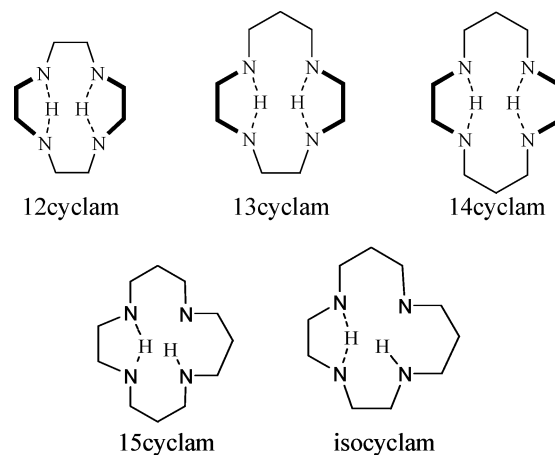
In their doubly protonated forms, these ligands have four free Lewis base sites available for coordination and thus are represented as squares in Figure 6. Only short lines with average slope have been added to the markers. Inspection of Figure 6 reveals that for these ligands at the 2+ stage the

increase on rate constants from ligands with three to four free sites is approximately 1 order of magnitude for Cu(II) and Ni(II). This value is significantly smaller than the regular increase of the rate constant for an additional free ligand site, which is approximately 3 orders of magnitude. This is evident for the step from two to three sites for Cu(II) and Ni(II) and from three to four free sites for Ni(II).

Presumably, the protonation in  $LH_2^{2+}$  occurs at the nitrogens in the macrocycle, thus leaving the pendant arms unprotonated. This seriously disrupts the system of hydrogen bridges, and additionally, for steric reasons, it is not possible to form hydrogen bridges between coordinated water molecules and both pendant arms of the ligand. The number of reasonably strong hydrogen bridges is substantially reduced, and this explains the small increase in the rate constants for the reaction of these ligands with the metal ions.

**Intramolecular Hydrogen Bridges in Doubly Protonated Cyclam-Type Macrocycles.** There is one additional group of striking exceptions to the trends identified so far. This group of significant outliers includes the doubly protonated forms of 12cyclam, 13cyclam, and 14cyclam in their reaction with Cu(II). The group of large solid diangles in Figure 6 represents the rate constants for these ligands that are significantly below the small diangles representing the “normal” case.

Closer inspection reveals that all three outlying macrocycles contain ethylenediamine moieties at opposite sides of the macrocycle, which allow strong intramolecular hydrogen bridges between two sets of adjacent N atoms, as drawn below. As a result, all four N atoms of the cyclam analogues are involved in internal hydrogen bonding, leaving much weaker interaction with the H atoms of coordinated water, and thus the outer-sphere stability constant is much lower. This behavior is not seen by larger 15cyclam and isocyclam.



The interpretation of this exceptionally strong intermolecular hydrogen bridging is supported by the reversed order of the third and fourth protonation constants of 14cyclam, which has been established by two separate and completely independent methods, calorimetry<sup>21</sup> and kinetics.<sup>6</sup> The doubly

(21) Micheloni, M.; Sabatini, A.; Paoletti, P. *J. Chem. Soc., Perkin Trans. 2* **1978**, 828–830.

protonated macrocyclic ring is highly stable as a result of the internal system of hydrogen bridges. Protonation with a third proton is unfavorable as this stable configuration has to be destroyed; hence, the protonation constant is low. Once the stable configuration has been lost, the fourth N atom is relatively exposed and the addition of a fourth proton is relatively easy and so the fourth protonation constant is higher than the third.

## Conclusion

Rate constants for the interaction of the partially protonated ligands 15ammac (10-methyl-1,4,8,12-tetraazacyclopentadecan-10-amine), 15cyclam (1,4,8,12-tetraazacyclopentadecane), and 15acmac (1,4,8,12-tetraazacyclopentadecan-10-carboxylic acid) with Cu(II) and Ni(II) in aqueous solution, determined here, are plotted jointly with a series of published rate constants for other macrocyclic ligands (see Figure 2). Two fairly consistent trends emerge: The higher the charge on the ligand, the slower the reaction with the metal ions, and ligands with a higher number of free donor sites react faster. Both observations are intuitively anticipated; they certainly do not contradict expectations.

The first observation is a straightforward electrostatic effect; the second is ascribed to an outer-sphere chelate effect. There is a fair amount of controversy and misunderstanding about the “chelate effect”, which stems from a loose definition of the expression. In this context we use the expression chelate effect in the sense that multidentate ligands form stronger complexes than monodentate ligands. The chelate effect has also been defined by the “observation”

that the equilibrium  $MA_2 + B-B \rightleftharpoons M(BB) + 2A$  lies on the right-hand side, where A is a monodentate and B–B represents a bidentate ligand. This statement, however, is imprecise, as the equilibrium constant is not dimensionless and the numerical value of the equilibrium constant depends on the dimensions chosen to represent concentration.<sup>2,22,23</sup>

The data used in our analysis are from a wide range of sources and acquired at different ionic strengths and temperatures. Nevertheless, the internal consistency of the arguments presents strong support for the interpretation of the observations as an outer-sphere chelate effect. The outer-sphere formation constants are small (as expected in aqueous solution); e.g.,  $K_{OS}$  for the interaction represented in Figure 4 is approximately 1 ( $\square$  in Figure 3). However, the presence of the outer-sphere complex is central in terms of driving the reaction. The results presented here are not limited to complexation reactions; they are of general relevance for essentially any interaction between ions in aqueous solution.

**Supporting Information Available:** Listings with the details of the kinetic runs (initial concentrations, pH ranges, and measurement times); outer-sphere complexation constants ( $\log K_{OS}$ ) for the interactions of the metal ions with ligands of charge 1+ to 5+ (table and graph); and published values for the rate constants for several other macrocyclic ligands with Cu(II) and Ni(II). This information is available free of charge via the Internet at <http://pubs.acs.org>.

IC0621143

(22) Schwarzenbach, G. *Helv. Chim. Acta* **1952**, 35, 2344–2359.

(23) Adamson, A. W. *J. Am. Chem. Soc.* **1954**, 76, 1578–1579.